Colloidal Interactions in Suspensions of Rods

Keng-hui Lin, John C. Crocker,* Ana C. Zeri,† and A. G. Yodh
Department of Physics and Astronomy, University of Pennsylvania, 209 S. 33rd Street, Philadelphia, Pennsylvania 19104-6396
(Received 13 April 2001; published 1 August 2001)

We report direct measurements of entropic interactions of colloidal spheres in suspensions of rodlike fd bacteriophage. We investigate the influence of sphere size, rod concentration, and ionic strength on these interactions. Although the results compare favorably with a recent calculation, small discrepancies reveal entropic effects due to rod flexibility. At high salt concentrations, the potential turns repulsive as a result of viral adsorption on the spheres and viral bridging between the spheres.

DOI: 10.1103/PhysRevLett.87.088301 PACS numbers: 82.70.Dd, 05.40.–a, 87.15.La

Colloidal mixtures exhibit a surprisingly diverse range of equilibrium phases depending on the size, shape, and concentration of suspension constituents [1]. In this paper we explore interactions between spheres in a suspension of rodlike particles. Such systems have captured the imagination of the physics community, exhibiting intriguing new phases not found in analogous liquid crystalline systems [2] and fluid-solid transitions at dramatically lower volume fractions [3] than corresponding colloid-particle and colloid-polymer systems [4]. The study of colloidal rods is also stimulated by rodlike molecules in biological systems, whose statistical-mechanical properties can influence their function inside cells [5].

A quantitative treatment of suspension stability and phase behavior requires a detailed understanding of the basic entropic interactions in suspension, as well as their modification by effects such as rod flexibility and solution ion concentration. Asakura and Oosawa (AO) were first to consider the entropic forces due to rods; they computed the attractive force between parallel plates in a solution of rigid thin rods [6]. Auvray extended the calculation to spheres using the Derjaguin approximation [7]. More recently, Yaman, Jeppesen, and Marques (YJM) accounted for sphere curvature beyond the Derjaguin approximation [8]. Calculations have also been extended to third order in rod concentration [9] and to other shapes [10–12]. The effects of such interactions have been explored theoretically in the phase diagrams of rod-sphere mixtures [1,13]. Still, there have been no direct measurements of rod-induced entropic interactions.

In this Letter, we describe the first interaction potential energy measurements between spheres in a suspension of monodisperse rodlike molecules, specifically fd bacteriophage virus. We measure the potential of the mean force between two spheres as a function of rod concentration and the ratio, a/L, of sphere radius to rod length. We compare our data to various theories [6–9]. Although the YJM model [8] might be expected to describe our data, we find significant deviations which we attribute to rod flexibility. The attractive depletion potential was unchanged over a relatively broad range of salt concentrations. At high salt, however, we found qualitatively different repulsive and harmonic potentials. These latter observations suggest that the ends of the fd virus can adhere to the particles, and can bridge between particles. Measurements in the bridged case provide mechanical information about single macromolecular rods.

Figure 1a illustrates the depletion interaction between two spheres of radius a immersed in a dilute suspension of thin rods of length L. When the center of a rod is located less than $L/2$ from the sphere surface (i.e., in the depletion zone, the hashed regions in Fig. 1), there are fewer possible orientations available to the rod, reducing its entropy. When the separation between sphere surfaces is less than L, the depletion zones around each sphere overlap, and the amount of accessible sample volume for unconstrained rod rotation increases. The total rod entropy increases in this case, inducing a depletion attraction between the spheres. The rod-induced depletion potential between spheres when $a \gg L$ has the form

$$U_{\mathrm{rod}}(h) = -\frac{\pi}{6} k_B T n_r a L^2 \left(1 - \frac{h}{L}\right)^3, \qquad (1)$$

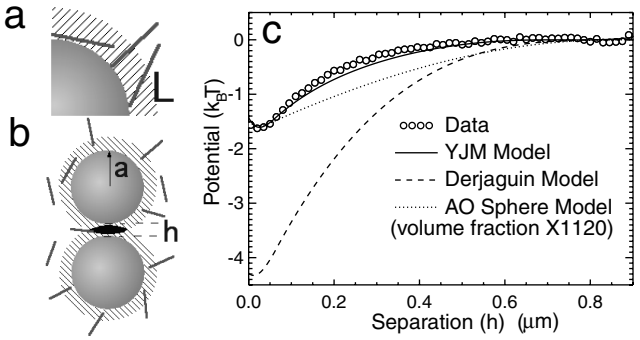

FIG. 1. The depletion attraction between two spheres. (a) Rods lose rotational degrees of freedom (and thus entropy) when their center lies in the depletion region (hashed regions) whose thickness extends $L/2$ beyond the surface of the large sphere. (b) When the large spheres approach each other, these depletion zones overlap (dark shading) and a volume, V_{overlap}, becomes accessible to the rods, increasing rod entropy and inducing an attractive force between the particles. (c) Comparison of typical data with three different models.

where n_r is the number density of the rods [9]; hereafter we will refer to this result as the Derjaguin model. This result contrasts with the well-known AO depletion potential due to a dilute gas of smaller spheres:

$$U_{\text{sphere}}(h) = -\frac{\pi}{2} k_B T n_s a \sigma^2 \left(1 - \frac{h}{\sigma}\right)^2, \qquad (2)$$

where σ is the small sphere diameter and n_s is the number density of small spheres. When $L = \sigma$ and $n_r = n_s$, the rod depletion potential has a more strongly curved shape and is shallower than a potential induced by the same number density of spheres. Still the rods occupy much less volume. In our case, the rods produce a depletion interaction more than 1000 times stronger than the same volume fraction of spherical depletants at the same volume fraction [3].

Many experiments involving rods and spheres violate the Derjaguin approximation. When $a \sim L$, there are fewer excluded orientations for a rod near a sphere than for a rod near a plate. Thus, the Derjaguin model overestimates the entropy gain from overlapped excluded volume. In general, exact analytic solutions for this geometry are not available. The authors of the YJM model [8] write the potential in the form

$$U_Y(h; a/L) = -k_B T n_r a L^2 K(h/L; a/L), \qquad (3)$$

and compute $K(h/L; a/L)$ numerically.

Before we describe our experiments and analysis in detail, a brief consideration of our data in the context of these three models seems worthwhile. A comparison between experiment and theory is shown in Fig. 1c. The circles are experimental data for 1.0 μm diameter silica particles in a dilute (0.7 mg/ml) solution of fd virus. The theory curves are computed with no free parameters and then numerically blurred to account for our instrument's spatial resolution. The Derjaguin model has an attraction at contact that is much too large. On the other hand, the YJM model has approximately the correct magnitude and shape. We will show below that the experimental deviations from the YJM model are likely due to the entropy associated with rod flexibility. We also plot the AO sphere model rescaled to have the correct depth, with $L = \sigma$. Notice that the rod depletion models are distinctly more curved than the spherical model.

In our experiments the rod molecules were fd bacteriophage. Fd virus are nearly monodisperse with length $L = 880$ nm, diameter $D = 6.6$ nm, molecular weight 1.64×10^7, and persistence length $l_P = 2.2$ μm. We used the protocol of Malik *et al.,* as shown in Ref. [14], to grow and purify fd. The final fd concentration was determined to better than 2% by UV spectrophotometry. The concentrations we used were well below the isotropic/nematic phase transition at about 10 mg/ml. The colloidal spheres were negatively charged silica beads of diameter 1.0 μm and 1.6 μm, with 2% polydispersity (Duke Scientific Inc.). A tiny volume fraction ($<10^{-6}$) of spheres was mixed with fd suspension and sealed into a microchamber. All the samples were pipetted gently to avoid breaking the virus.

Our measurements were performed with a line-scanned optical tweezer (50 mW, $\lambda = 1053$ nm, $NA = 1.3$) [15]. Briefly, the two silica spheres were trapped in a one-dimensional optical potential generated by scanning a tightly focused laser beam back and forth along a line at 180 Hz. The line trap was focused more than 4 μm away from the sample chamber's cover glass to minimize possible wall effects. The two spheres in the trap shared a roughly harmonic potential along the scan direction and were strongly confined in the other two dimensions. For each potential measurement, the spheres' thermal motion was followed by bright-field video microscopy and recorded on a S-VHS deck for an hour; subsequent digitization yielded 2×10^5 images. Center-to-center separations were estimated by the in-plane distance between the sphere images' brightness-weighted centroids [16]. We employ an algorithm which largely corrects for the overlap of the spheres' diffraction blurred images [15].

The interparticle potential $U(h)$ was calculated from the measured probability distribution of sphere contact separations, $P(h)$, using the Boltzmann relation $P(h) \propto \exp[-U(h)/k_B T]$. We made one measurement with rods and another without rods under the same optical and chemical conditions; this enabled us to isolate the potential due to the rods from other contributions. To quantitatively compare the observed data with a model potential, we first convert the model to a probability distribution, $P(h)$, numerically convolve it with a Gaussian kernel to simulate our instrumental resolution, and then convert it back to a potential by taking the logarithm. The $P(h)$ distributions for hard spherelike control measurements were well fit by a step edge convolved by a Gaussian with a 30 nm half width. We use that value for the blurring kernel in all model comparisons. The energy resolution of $0.05 k_B T$ is set by counting statistics.

Figure 2 displays the resulting potentials for all measured fd concentrations and two different sizes of colloidal spheres. As expected, we see that, for the same rod concentration, the depletion attraction is stronger between the larger pair of spheres. Also shown in the figure (dotted curves) is the resolution-blurred YJM model with exact input parameters ($L = 880$ nm and number density). The measured potential, however, is more strongly curved and systematically weaker than the theoretical model. We believe this discrepancy is due to rod flexibility. Even though the persistence length $l_P = 2.2$ μm of the rods is much longer than their contour length of 880 nm, bending and undulations of the virus make them appear shorter on average. The mean-squared end-to-end distance, $\langle R^2 \rangle$, is given by the Kratky-Porod (KP) expression [17],

$$\langle R^2 \rangle = L l_p + \tfrac{1}{2} l_p^2 (e^{-2L/l_p} - 1). \qquad (4)$$

For fd, the root-mean-squared (RMS) end-to-end length is $R_{\text{RMS}} = 0.78$ μm. We substitute R_{RMS} for L in the

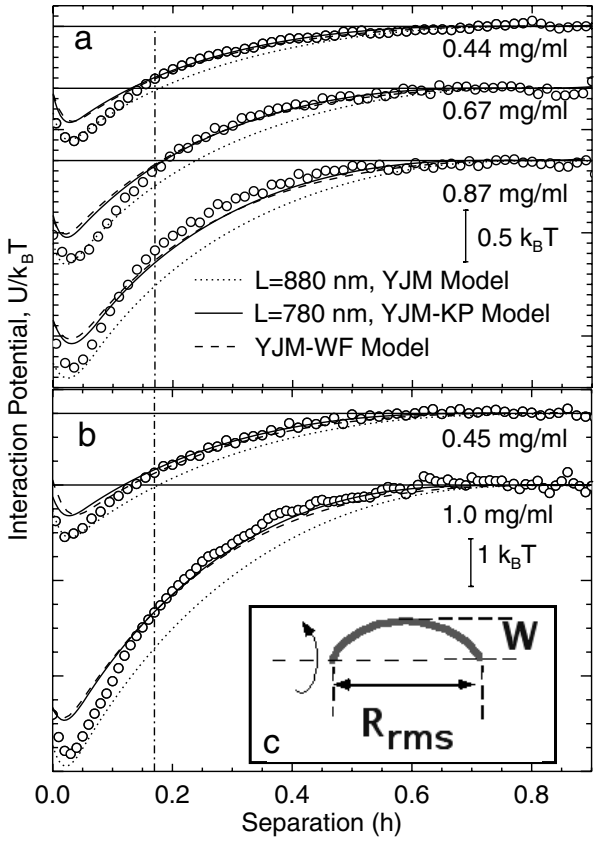

FIG. 2. Interaction potential between pairs of (a) 1.0 μm and (b) 1.6 μm silica spheres in a suspension of fd virus at varying concentration. The dotted (solid) lines are generated by the YJM model with $L = 880$ nm ($L = 780$ nm). The dashed lines are generated by the YJM model with length distribution. This is essentially indistinguishable from the $L = 780$ nm model. The dash-dotted vertical line indicates $W = 0.17$ μm. (c) This shows a bent rod with end-to-end separation R, transverse amplitude W, and a new rotation axis.

YJM model yielding the solid curves in Fig. 2. The rod-bending modified YJM curves (YJM-KP) provide good agreement at large separations. At contact, however, the data is $\sim$20% deeper than the YJM-KP model.

The fact that a polydisperse rod suspension can have a more strongly curved depletion potential leads us to consider the actual end-to-end distance distribution $G(r)$ for fd. Using the $G(r)$ from the calculation of Wilhelm and Frey (WF) [18], we computed a new depletion potential by numerically superposing YJM models [Eq. (3)] with different L, weighted by $G(r)$. The results (dashed lines, YJM-WF) were barely distinguishable from the YJM-KP model, suggesting that the distribution of effective lengths does not explain the entropic discrepancy at short separation. Similar calculations demonstrated that the data could not be explained because a fraction of the virus was broken during storage and handling.

The repeatable discrepancy at small h reveals entropic contributions from another degree of freedom in the system. Flexible rods undulate in thermal equilibrium, and entropy is associated with these degrees of freedom. For example, the bent rods have more rotational degrees of freedom than straight rods: bent rods explore physically distinguishable configurations when they rotate about the axis connecting their ends. These effects become significant only when the sphere surface separation is less than the typical transverse extent, W, of the rods. The relative increase of suspension entropy for closely separated spheres is thus greater for flexible rods than for rigid rods with equivalent end-to-end length. To estimate W, we consider a rod bent into a circular arc with end-to-end separation 0.78 μm and contour length 0.88 μm (Fig. 2c). In this case $W = 0.17$ μm (dash-dotted line), roughly the separation length scale at which our experimental data deviate from the YJM-KP model. More theoretical work is required to quantitatively model the entropic mechanism we have detected. We can rule out dispersion force effects [19] as a possible mechanism; they are smaller, they would produce a deviation with the opposite sign, and they do not predict a natural crossover at $h = 0.17$ μm.

We next explored how the variation of the effective rod diameter alters the depletion potential. To this end, we changed the Debye screening length, κ^{-1}, from 16 to 3 nm, which in turn modified the effective rod diameter $D_{\text{eff}} = D + 2\kappa^{-1}$, changing the ratio L/D of the rods. Specifically, we varied the NaCl concentration between 0 and 10 mM at constant 2 mM sodium borate and pH 8.0. Our measurements (data not shown) found no change in the depletion attraction, suggesting that the thin rod approximation holds in our system. Moreover, this confirms that the electrostatic interactions between the spheres and the rods are insignificant.

At still higher salt concentrations (i.e., $>$20 mM), the spheres in a pure buffer solution become sticky and the sphere-sphere interaction in rod solution changes dramatically, becoming repulsive. We speculate that this repulsion is due to the fd molecules adhering (perhaps end on) to the particle surfaces. The major coat protein along the fd cylinder is highly negatively charged, making adsorption there more difficult than for the ends. The composition of the ends is different; one end of fd is the G3P minor coat protein whose function is to grab the pilus of *E. coli*, the other end is hydrophobic.

In Figs. 3(a) and 3b we illustrate the two types of repulsive interactions we have observed—linear and harmonic. In Fig. 3(a) we exhibit two potentials. Both decay in a linear fashion with increasing separation and have a range approximately equal to the length of the virus, L. Although both of these potentials are repulsive and have the same range, the force between the spheres is quite different in the two cases, i.e., (x) 29.4 $\pm$ 0.03 femtoNewton (fN) and (y) 5.9 $\pm$ 0.04 fN. One explanation for this difference is that a different number of viruses are bound to the particles in each case. In Fig. 3(b) we observe a more harmonic interaction, which we hypothesize is due to fd bridging between the spheres. The maximum separation between

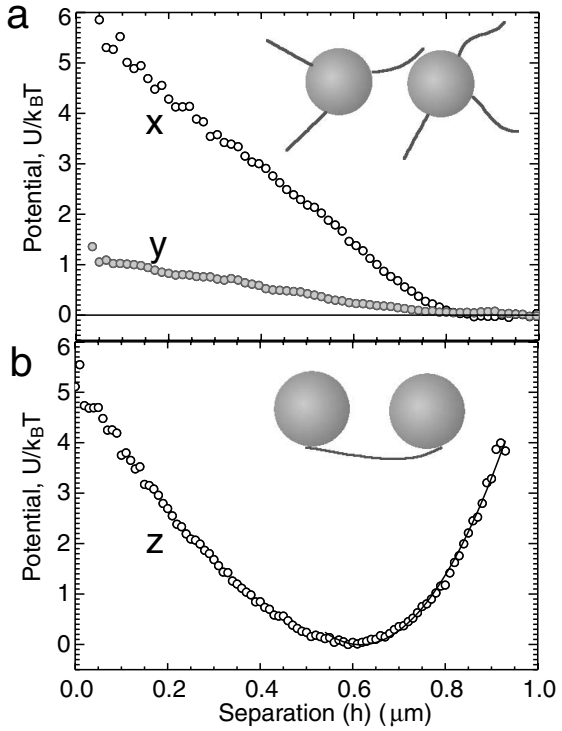

FIG. 3. x is derived from samples with 2 mM sodium borate + 10 mM NaCl, 0.5 mg/ml fd, and the two other potentials are derived from samples with 10 mM TE + 20 mM NaCl, 0.2 mg/ml fd, and (a) steric repulsion between particles due to the "rod brush." (b) Harmonic interaction potential due to bridging of fd between two spheres.

the spheres was L and the potential minimum occurred at $h = 0.57\ \mu$m. For $h < 0.57\ \mu$m, the potential is approximately linear as in Fig. 3a. For $h > 0.57\ \mu$m, the potential is well fit by a quadratic form, giving a spring constant of $84 k_B T/\mu\text{m}^2$. Calculation of these harmonic interactions will require further effort. Still, this methodology provides a new window into the equilibrium mechanical properties of single macromolecular rods.

To conclude, we have presented the first measurements of interactions between particles in rodlike suspensions. Our results are well approximated by the YJM-KP model [8], which takes both sphere and rod curvature into account. The remaining deviations at small separation are due to non-negligible contributions from the entropy of bent rod conformations, which have not been considered in the literature. We also observed steric repulsion and bridging effects at high salt. In total, these observations can be used to understand the phase behavior and stability of these and related suspensions, and to gain insight into the mechanical behavior of macromolecules.

We are grateful to Dr. Stanley Opella's group for teaching us to grow fd virus. We thank Randy Kamien, Alex Levine, Paul Janmey, and particularly Carlos Marques for useful discussions. Support was provided by the NSF through Grant No. DMR 99-71226 and the MRSEC Grant No. DMR 00-79909. Dr. Opella's group acknowledge NIH Grant No. R37GM24266.

*Current address: Department of Applied Physics, Caltech, Mail Code 128-95, Pasadena, California 91125.
†Current address: Department of Chemistry and Biochemistry, University of California at San Diego, La Jolla, California 92093.

[1] G. A. Vliegenthart and H. N. W. Lekkerkerker, J. Chem. Phys. **111**, 4153 (1999).
[2] M. Adams, Z. Dogic, S. L. Keller, and S. Fraden, Nature (London) **393**, 349 (1998).
[3] G. H. Koemderoml *et al.,* Langmuir **15**, 4693 (1999); G. A. Vliegenthart, A. van Blaaderen, and H. N. W. Lekkerkerker, Faraday Discuss. **112**, 173 (1999).
[4] S. M. Ilett, A. Orrock, W. C. K. Poon, and P. N. Pusey, Phys. Rev. E **51**, 1344 (1995).
[5] A. R. Hemsley and P. C. Griffiths, Philos. Trans. R. Soc. London A **358**, 547 (2000).
[6] S. Asakura and F. Oosawa, J. Polym. Sci. **33**, 183 (1958).
[7] L. Auvray, J. Phys. (Paris) **42**, 79 (1981).
[8] K. Yaman, C. Jeppesen, and C. M. Marques, Europhys. Lett. **42**, 221 (1998).
[9] Y. Mao, M. E. Cates, and H. N. W. Lekkerkerker, J. Chem. Phys. **106**, 3721 (1997); Y. Mao, M. E. Cates, and H. N. W. Lekkerkerker, Phys. Rev. Lett. **75**, 4548 (1995).
[10] P. van der Schoot, J. Chem. Phys. **20**, 9132 (2000).
[11] M. Piech and J. Y. Walz, J. Colloid Interface Sci. **232**, 86 (2000).
[12] M. Triantafillou and R. D. Kamien, Phys. Rev. E **59**, 564 (1999).
[13] Z. Dogic, D. Frenkel, and S. Fraden, Phys. Rev. E **62**, 3925 (2000).
[14] B. K. Kay, J. Winter, and J. McCafferty, *Phage Display of Peptides and Proteins* (Academic Press, London, 1996).
[15] J. C. Crocker, J. A. Matteo, A. D. Dinsmore, and A. G. Yodh, Phys. Rev. Lett. **82**, 4352 (1999); R. Verma, J. C. Crocker, T. C. Lubensky, and A. G. Yodh, Phys. Rev. Lett. **81**, 4004 (1998); R. Verma, J. C. Crocker, T. C. Lubensky, and A. G. Yodh, Macromolecules **33**, 177 (2000).
[16] J. C. Crocker and D. G. Grier, J. Colloid Interface Sci. **179**, 298 (1996).
[17] O. Kratky and G. Porod, G. Recl. Trav. Chim. **68**, 1106 (1949).
[18] J. Wilhelm and E. Frey, Phys. Rev. Lett. **77**, 2581 (1996).
[19] C. Bechinger *et al.*, Phys. Rev. Lett. **83**, 3960 (1999).